



Magnetic field and internal heat generation effects on the free convection in a rectangular cavity filled with a porous medium

T. Grosan^a, C. Revnic^b, I. Pop^{a,*}, D.B. Ingham^c

^aBabes-Bolyai University, Department of Applied Mathematics, CP 253, R-3400 Cluj, Romania

^bUniversity of Medicine and Pharmacy "Iuliu Hatieganu", Faculty of Pharmacy, Cluj, Romania

^cCentre for Computational Fluid Dynamics, University of Leeds, Leeds LS2 9JT, UK

ARTICLE INFO

Article history:

Received 15 August 2008

Available online 1 October 2008

Keywords:

Porous media

Natural convection

Heat generation

MHD

ABSTRACT

A numerical investigation of the steady magnetohydrodynamics free convection in a rectangular cavity filled with a fluid-saturated porous medium and with internal heat generation has been performed. A uniform magnetic field, inclined at an angle γ with respect to the horizontal plane, is externally imposed. The values of the governing parameters are the inclined angle $\gamma = 0, \pi/6, \pi/4$ and $\pi/2$, Hartmann number $Ha = 0, 1, 5, 10$ and 50 , Rayleigh number $Ra = 10, 100, 10^3$ and 10^5 , and the aspect ratio $a = 0.01, 0.2, 0.5$ and 1 (square cavity). It is shown that the intensity of the core convection is considerably affected by the considered parameters. It is also found that the local Nusselt number Nu_γ decreases on the bottom wall as γ increases (magnetic field changes its direction from the horizontal to the vertical direction) and vice versa for the top wall of the cavity. The reported results are in good agreement with the available published work in the literature.

© 2008 Elsevier Ltd. All rights reserved.

1. Introduction

Natural convective heat transfer in viscous fluids and fluid-saturated porous media has occupied the central stage in many fundamental heat transfer analyses and has received considerable attention over the last few decades. This interest is due to its wide range of applications in, for example, packed sphere beds, high performance insulation for buildings, chemical catalytic reactors, grain storage and such geophysical problems as frost heave. Porous media are also of interest in relation to the underground spread of pollutants, solar power collectors, and to geothermal energy systems. The literature concerning convective flow in porous media is abundant and representative studies in this may be found in the recent books by Nield and Bejan [1], Ingham and Pop [2], Vafai [3], Bejan et al. [4], Pop and Ingham [5], de Lemos [6] and Vadasz [7]. Further, a valuable reference on convective fluids in cavities filled with viscous fluids can be found in the recent book by Martynenko and Khramtsov [8]. Natural convection in enclosures in which internal heat generation is present is of prime importance in certain technological applications. Examples are post-accident heat removal in nuclear reactors and geophysical problems associated with the underground storage of nuclear waste, among others (Acharya and Goldstein [9], Ozoe and Maruo [10], Lee and Goldstein [11], Fusegi et al. [12], Venkatachalappa and Subbaraya [13], Shim and Hyun [14], Hossain and Wilson [15]).

The present paper investigates the effect of a magnetic field on the steady free convection in a rectangular cavity filled with a porous medium saturated with an electrically conducting fluid. This type of problem arises in geophysics when a fluid saturates the earth's mantle in the presence of a geomagnetic field. Natural convection flow in the presence of a magnetic field in an enclosure filled with a viscous and incompressible fluid has been studied by Garandet et al. [16], Alchar et al. [17], Kanafer and Chamka [18], Chamkha and Al-Naser [19], Mahmud et al. [20], Hossain and Ress [21], Hossain et al. [22], and Ece and Büyük [23]. However, there are very few studies on the natural convection of a conducting fluid saturating a porous medium in the presence of a magnetic field in an enclosure. To the best of our knowledge, the first investigation of this problem is due to Alchar et al. [17] who considered the stability of a conducting fluid saturating a porous medium in the presence of a uniform magnetic field using the Brinkman model. However, some comments on the MHD convection in a porous medium have been done very recently by Nield [24]. Also a very recent paper by Barletta et al. [25] has studied the mixed convection with heated effect in a vertical porous annulus with the radially varying magnetic field.

2. Mathematical model

In this paper, we consider the steady natural convection flow in a rectangular cavity filled with an electrically conducting fluid-saturated porous medium with internal heat generation. We assume

* Corresponding author. Tel.: +40 264 594 315; fax: +40 264 591 906.
E-mail address: pop.ioan@yahoo.co.uk (I. Pop).

Nomenclature

a	aspect ratio	T_0	temperature of the vertical wall (K)
\mathbf{B}	applied magnetic field (Wb m^{-2})	x	dimensional Cartesian coordinate along the bottom wall (m)
c_p	specific heat at constant pressure ($\text{kJ kg}^{-1} \text{K}^{-1}$)	y	dimensional Cartesian coordinate along the left vertical wall (m)
\mathbf{g}	gravitational acceleration vector (m s^{-2})	X, Y	dimensionless Cartesian coordinates
Ha	Hartmann number	<i>Greek symbols</i>	
h	height of the cavity (m)	α_m	effective thermal diffusivity ($\text{m}^2 \text{s}^{-1}$)
k	thermal conductivity ($\text{W m}^{-1} \text{K}^{-1}$)	β	coefficient of thermal expansion (K^{-1})
K	permeability of the porous medium (m^2)	γ	angle of inclination to the horizontal of applied magnetic field (rad)
l	width of the cavity (m)	μ	dynamic viscosity ($\text{kg m}^{-1} \text{s}^{-1}$)
Nu	mean Nusselt number	θ	dimensionless temperature
Nu_y	local Nusselt number	ρ	fluid density (kg m^{-3})
q_0'''	heat generation (W m^{-3})	ρ_0	reference density (kg m^{-3})
Ra	Rayleigh number	σ	electrical conductivity ($\Omega^{-1} \text{m}^{-1}$)
u, v	velocity components along the x - and y -directions, respectively (m s)		
\mathbf{V}	velocity vector (m s^{-1})		

that the enclosure is permeated by a uniform inclined magnetic field. The geometry and the Cartesian coordinate system are schematically shown in Fig. 1, where the dimensional coordinates x and y are measured along the horizontal bottom wall and normal to it along the left vertical wall, respectively. The height of the cavity is denoted by h and the width by l . Further, the angle of inclination of the magnetic field \mathbf{B} from the horizontal plane and measured positively in the counterclockwise direction is denoted by γ . It is assumed that the vertical walls are maintained at a constant temperature T_0 , while the horizontal walls are adiabatic. A uniform source of heat generation in the flow region with a constant volumetric rate of q_0''' (W m^{-3}) is also considered. Further, it is assumed that the effect of buoyancy is included through the well-known Boussinesq approximation. The viscous, radiation and Joule heating effects are neglected. The resulting convective flow is governed by the combined mechanism of the driven buoyancy force, internal

heat generation and the retarding effect of the magnetic field. The magnetic Reynolds number is assumed to be small so that the induced magnetic field can be neglected compared to the applied magnetic field.

Under the above assumptions, the conservation equations for mass, momentum under the Darcy approximation, energy and electric transfer are given by

$$\nabla \cdot \mathbf{V} = 0 \quad (1)$$

$$\mathbf{V} = \frac{K}{\mu} (-\nabla p + \rho \mathbf{g} + \mathbf{I} \times \mathbf{B}) \quad (2)$$

$$(\mathbf{V} \cdot \nabla) T = \alpha_m \nabla^2 T + \frac{q_0'''}{\rho_0 c_p} \quad (3)$$

$$\nabla \cdot \mathbf{I} = 0 \quad (4)$$

$$\mathbf{I} = \sigma (-\nabla \phi + \mathbf{V} \times \mathbf{B}) \quad (5)$$

$$\rho = \rho_0 [1 - \beta(T - T_0)] \quad (6)$$

where \mathbf{V} is the fluid velocity vector, T is the fluid temperature, p is the pressure, \mathbf{B} is the external magnetic field, \mathbf{I} is the electric current, ϕ is the electric potential, \mathbf{g} is the gravitational acceleration vector, K is the permeability of the porous medium, α_m is the effective thermal diffusivity, ρ is the density, μ is the dynamic viscosity, β is the coefficient of thermal expansion, c_p is the specific heat at constant pressure, σ is the electrical conductivity, ρ_0 is the reference density and $-\nabla \phi$ is the associated electric field. As discussed by Garandet et al. [16], Eqs. (4) and (5) reduce to $\nabla^2 \phi = 0$. The unique solution is $\nabla \phi = 0$ since there is always an electrically insulating boundary around the enclosure. Thus, it follows that the electric field vanishes everywhere (see, Alchaar et al. [17]).

Eliminating the pressure term in Eq. (2) in the usual way, the governing equations (1)–(3) can be written as

$$\frac{\partial u}{\partial x} + \frac{\partial v}{\partial y} = 0 \quad (7)$$

$$\frac{\partial u}{\partial y} - \frac{\partial v}{\partial x} = -\frac{gK\beta}{\nu} \frac{\partial T}{\partial x} + \frac{\sigma KB_0^2}{\mu} \left(-\frac{\partial u}{\partial y} \sin^2 \gamma + 2 \frac{\partial v}{\partial y} \sin \gamma \cos \gamma + \frac{\partial v}{\partial x} \cos^2 \gamma \right) \quad (8)$$

$$u \frac{\partial T}{\partial x} + v \frac{\partial T}{\partial y} = \alpha_m \left(\frac{\partial^2 T}{\partial x^2} + \frac{\partial^2 T}{\partial y^2} \right) + \frac{q_0'''}{\rho c_p} \quad (9)$$

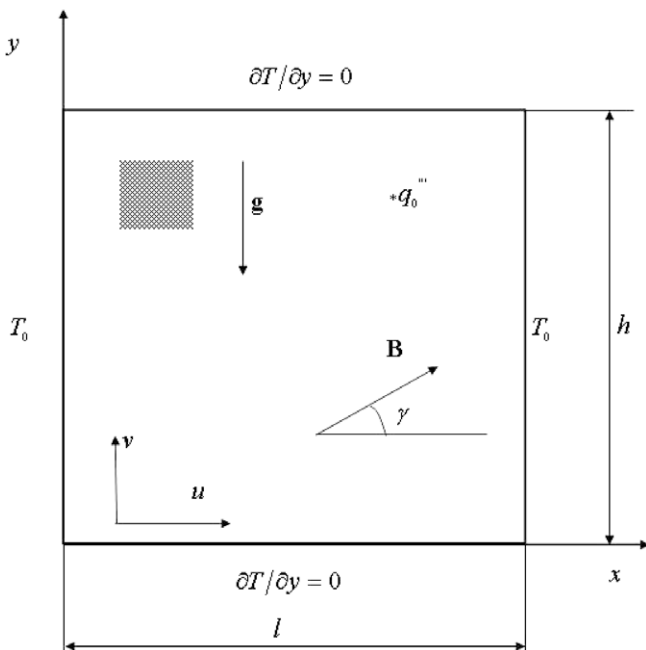


Fig. 1. Geometry of the problem and coordinate system.

which has to be solved subject to the boundary conditions

$$\begin{aligned}
 u = 0, \quad T = T_0 \text{ at } x = 0 \text{ and } x = l, \quad 0 \leq y \leq h \\
 v = 0, \quad \frac{\partial T}{\partial y} = 0 \text{ at } y = 0 \text{ and } y = h, \quad 0 \leq x \leq l
 \end{aligned} \tag{10}$$

where B_0 is the magnitude of \mathbf{B} and ν is the kinematic viscosity of the fluid. Further, we introduce the following non-dimensional variables

$$X = \frac{x}{l}, \quad Y = \frac{y}{h}, \quad U = \frac{h}{\alpha_m} u, \quad V = \frac{l}{\alpha_m} v, \quad \theta = \frac{T - T_0}{(q_0'' l^2 / k)} \tag{11}$$

where k is the thermal conductivity. Introducing the stream function ψ defined as $U = \partial\psi/\partial Y$ and $V = -\partial\psi/\partial X$, and using expressions (11) in Eqs. (7)–(9), we obtain the following partial differential equations in non-dimensional form:

$$\begin{aligned}
 \frac{\partial^2 \psi}{\partial X^2} + a^2 \frac{\partial^2 \psi}{\partial Y^2} = -Ra \frac{\partial \theta}{\partial X} \\
 - Ha^2 \left(a^2 \frac{\partial^2 \psi}{\partial Y^2} \sin^2 \gamma + 2a \frac{\partial^2 \psi}{\partial X \partial Y} \sin \gamma \cos \gamma + \frac{\partial^2 \psi}{\partial X^2} \cos^2 \gamma \right) \tag{12}
 \end{aligned}$$

$$\frac{\partial^2 \theta}{\partial X^2} + a^2 \frac{\partial^2 \theta}{\partial Y^2} + 1 = a \left(\frac{\partial \psi}{\partial Y} \frac{\partial \theta}{\partial X} - \frac{\partial \psi}{\partial X} \frac{\partial \theta}{\partial Y} \right) \tag{13}$$

which have to be solved subject to the boundary conditions

$$\begin{aligned}
 \psi = 0, \quad \theta = 0, \text{ at } X = 0 \text{ and } X = 1, \quad 0 \leq Y \leq 1 \\
 \psi = 0, \quad \frac{\partial \psi}{\partial Y} = 0, \quad \frac{\partial \theta}{\partial Y} = 0 \text{ at } Y = 0 \text{ and } Y = 1, \quad 0 \leq X \leq 1
 \end{aligned} \tag{14}$$

where $a = l/h$ is the aspect ratio of the cavity, $Ra = gK\beta\Delta TH/\alpha\nu$ is the Rayleigh number and $Ha = \sigma KB_0^2/\mu$ is the Hartmann number for the porous medium. It should be mentioned that $\gamma = 0$ corresponds to a horizontal magnetic field and $\gamma = \pi/2$ corresponds to a vertical magnetic field, respectively.

Once we know the temperature we can obtain the rate of heat transfer from each of the vertical walls, which are given in terms of the local Nusselt number Nu_Y which is defined as

$$Nu_Y = - \left(\frac{\partial \theta}{\partial X} \right)_{X=0} \tag{15}$$

3. Numerical method and validation

To obtain the numerical solution of Eqs. (12) and (13) a central finite-difference scheme was used and the system of discretized equations has been solved using a Gauss–Seidel iteration technique. The unknowns θ and ψ were calculated iteratively until the following criteria of convergence was fulfilled:

Table 1
Accuracy test for $Ra = 10^3$, $Ha = 0$ and $a = 1$

Nodes	$\psi(0.24, 0.24)$	$\theta(0.24, 0.24)$
26 × 26	2.6368	0.0389
51 × 51	2.5987	0.0384
101 × 101	2.5800	0.0382
201 × 201	2.5707	0.0381
Richardson extrapolation	2.5614	0.0380

Table 2
Comparison of ψ_{\max} and θ_{\max} for $Ha = 0$ and $a = 0.5$

Ra	Haajizadeh et al. [27]		Present (Richardson extrapolation)	
	ψ_{\max}	θ_{\max}	ψ_{\max}	θ_{\max}
10	0.078	0.130	0.079	0.127
10 ³	4.880	0.118	4.833 (4.832)	0.116 (0.116)

$$|\max [\chi_{\text{new}}(i, j) - \chi_{\text{old}}(i, j)]| \leq \varepsilon \tag{16}$$

where χ represents the temperature or the stream function and ε is the convergence criteria. In all the results presented in this paper, $\varepsilon = 10^{-7}$ was found to be sufficiently small such that any smaller value produced results which were graphically the same. In order to choose the size of the grid, accuracy tests using the finite difference method and Richardson extrapolation [26] for mesh sensitivity analysis were performed for $Ra = 10^3$, $Ha = 0$, and aspect ratio $a = 1$, using three sets of grids: 26×26 , 51×51 , 101×101 and 201×201 as shown in Table 1. Reasonably good agreement was found between the 51×51 and 101×101 grids and therefore the grid used in this problem was 101×101 and these give accurate results for $Ra \leq 10^3$. We have also found that 201×201 grids give accurate results for $Ra \leq 10^5$.

Further, in order to verify the accuracy of the code we compared the obtained results for the case when the magnetic field is absent ($Ha = 0$), $a = 0.5$ and $Ra = 10$ and 10^3 , respectively, with those obtained by Haajizadeh et al. [27]. These results are shown in Table 2. It can be concluded from this table that the results are in good agreement and we can be confident that the present analysis and the code used are correct.

4. Analytical solution

For small values of a ($a \ll 1$), the solution of Eqs. (12) and (13) is given by the leading order terms, $\psi = \psi_0(x)$ and $\theta = \theta_0(x)$, see Mandar et al. [29]

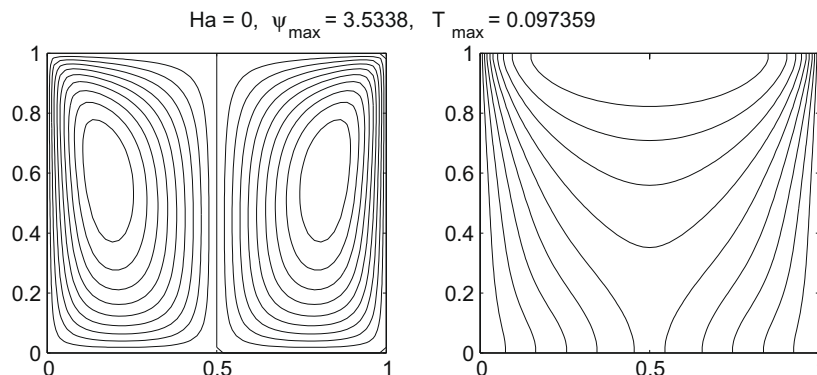


Fig. 2. Streamlines and isotherms for $Ra = 10^3$, $Ha = 0$ when the magnetic field is in horizontal direction ($\theta = 0^\circ$).

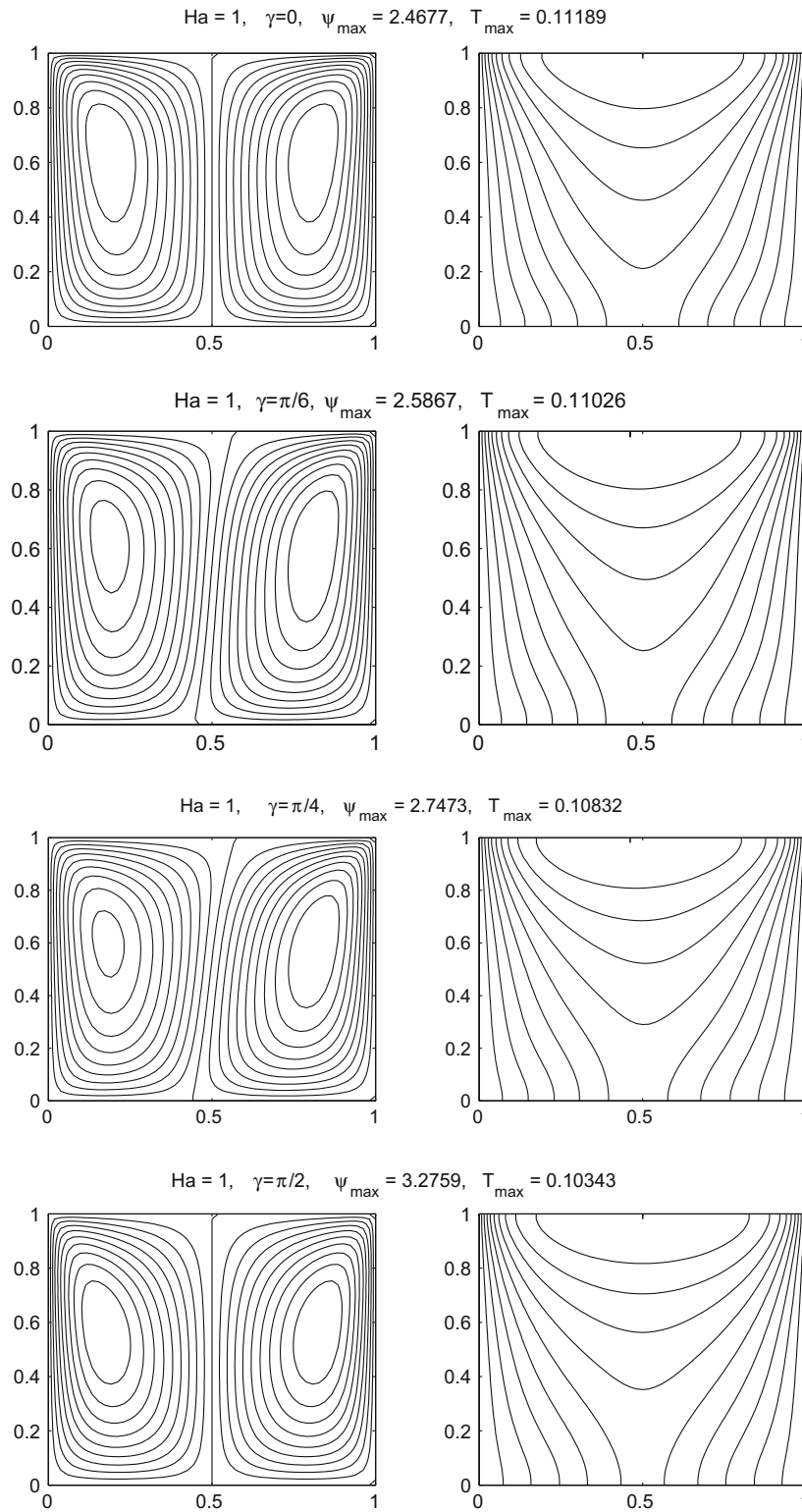


Fig. 3. Streamlines and isotherms for $Ra = 10^3$, $Ha = 1$ and for different values of γ .

$$(1 + Ha^2 \cos^2 \gamma) \frac{\partial^2 \psi_0}{\partial X^2} = -Ra \frac{\partial \theta_0}{\partial X} \quad (17)$$

$$\frac{\partial^2 \theta_0}{\partial X^2} + 1 = 0 \quad (18)$$

with the boundary conditions

$$\psi_0 = \theta_0 = 0 \text{ at } X = 0 \text{ and } X = 1 \quad (19)$$

On solving Eqs. (17) and (18) with the boundary conditions (19), we obtain

$$\theta_0(X) = \frac{X(1-X)}{2} \quad (20)$$

$$\psi_0(X) = \frac{Ra}{2(1 + Ha^2 \cos^2 \gamma)} \left(\frac{1}{6}X - \frac{1}{2}X^2 + \frac{1}{3}X^3 \right).$$

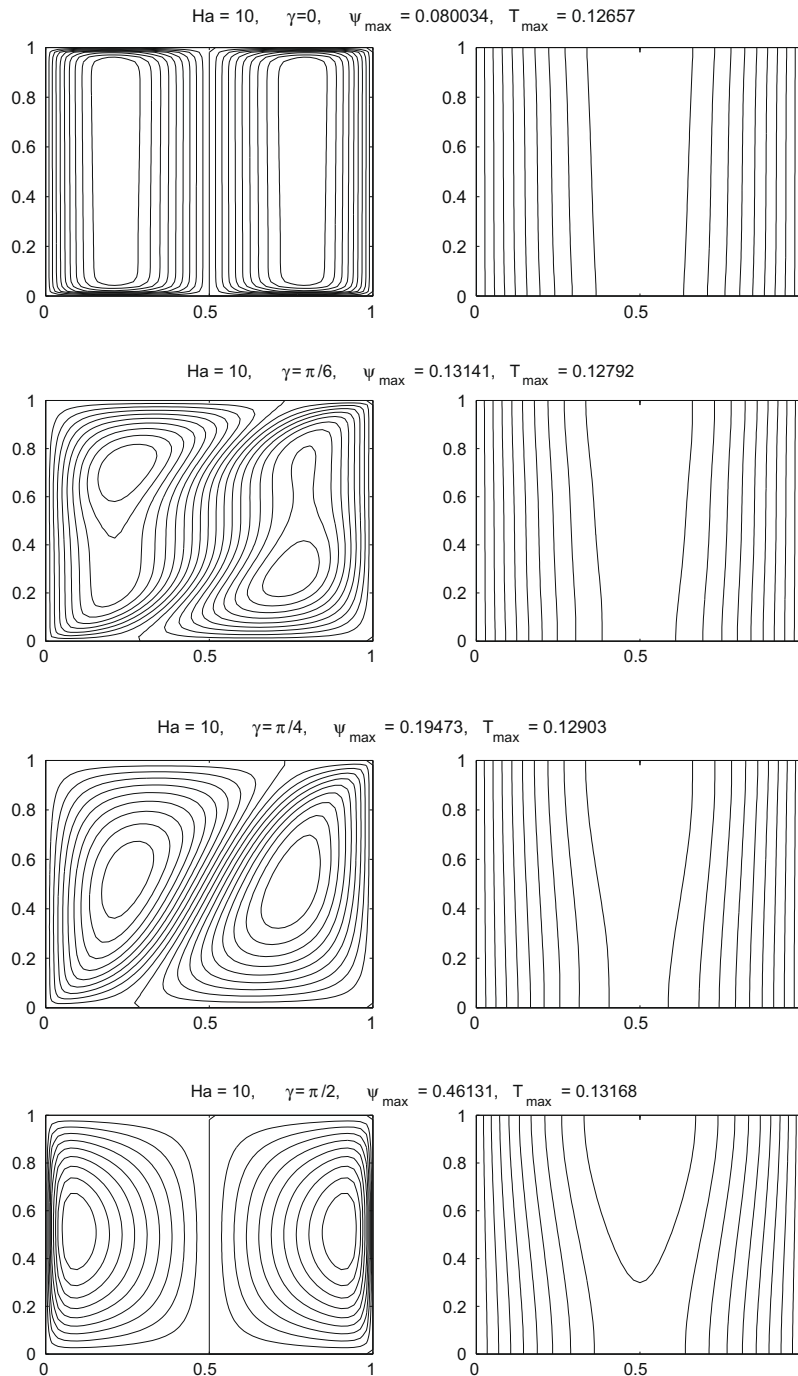


Fig. 4. Streamlines and isotherms for $Ra = 10^3$, $Ha = 10$ and for different values of γ .

5. Results and discussion

In this section, we present numerical results for the streamlines, isotherms and velocity profiles on the left wall, for various values of the magnetic field parameter Ha , inclination angle γ of the magnetic field and the Rayleigh number Ra . In addition, the local Nusselt numbers Nu_γ have been calculated. Figs. 2–6 show plots of the streamlines and isotherms for an aspect ration $a = 1$, Rayleigh number $Ra = 10^3$ and 10^5 , magnetic field parameter $Ha = 0, 1, 10$ and 50 and values of the inclined angle $\gamma = 0, \pi/6, \pi/4$ and $\pi/2$. It is seen from these figures that the intensity of the convection in the core is considerably affected by the magnetic field. A weak convective motion with a bicellular structure is induced, see Fig. 2.

two cells are symmetrical with respect to the central plane according to the value of γ . It is also observed that these two cells rotate for $\gamma = \pi/6$ and $\pi/4$. It is seen from Fig. 2 that the pattern of the streamlines and isotherms are similar to those predicted by Haajizadeh et al. [27]. On the other hand, Fig. 3 illustrates that for relative small values of Ha ($Ha = 1$) the maximum stream function increases and the maximum temperature decreases as γ increases. However, for larger values of Ha ($Ha \gg 1$) the maximum of both the stream function and the temperature increase as γ increases. Therefore, the presence of the magnetic force tends to accelerate the fluid motion inside the cavity when the direction of the magnetic field changes from the horizontal to the vertical direction. Further, for $Ra = 10^3$ and higher values of Ha , the isotherms are

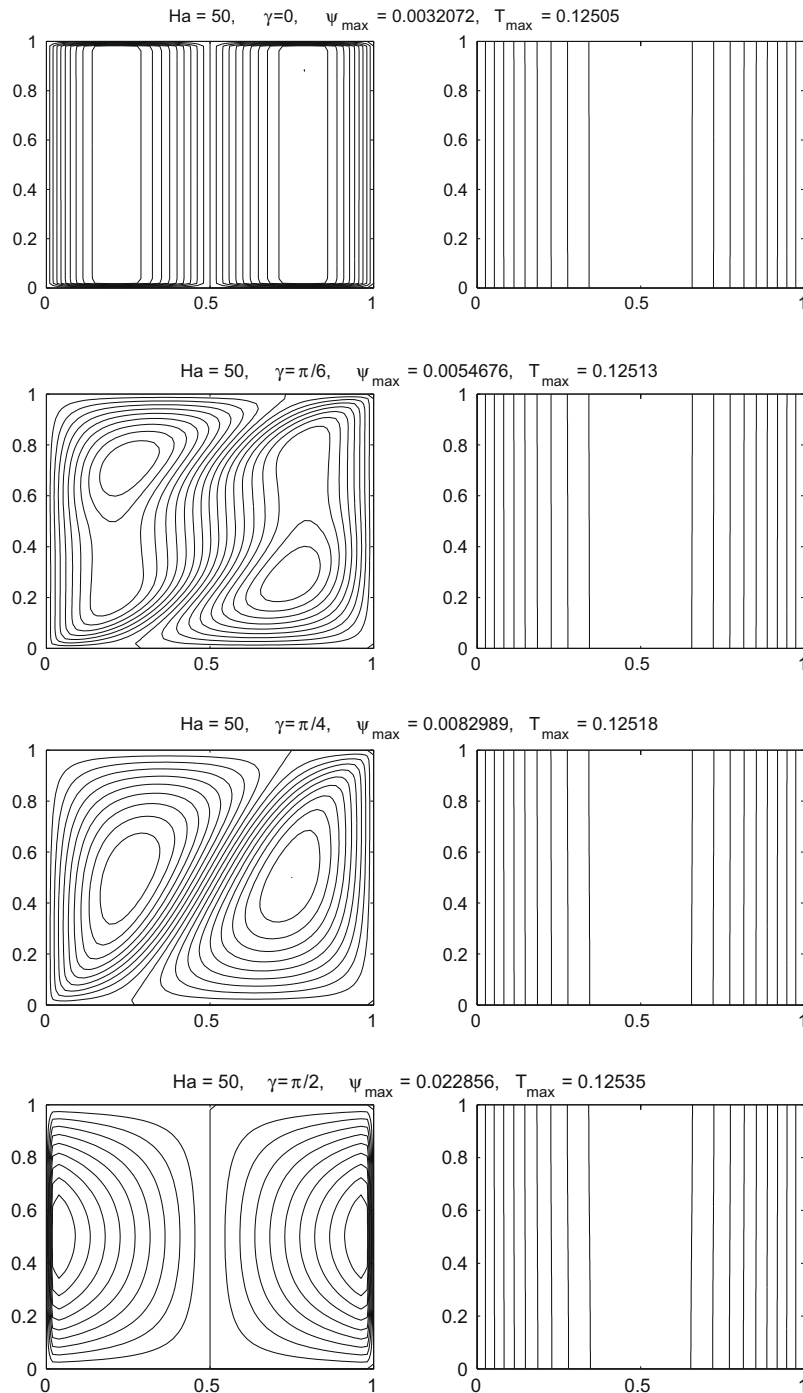


Fig. 5. Streamlines and isotherms for $Ra = 10^3$, $Ha = 50$ and for different values of γ .

almost parallel and this implies that conduction is dominant, see Figs. 4 and 5. Also, these figures show that when the magnetic field is horizontal ($\gamma = 0$) and $Ra = 10^3$ the core vortex is elongated vertically as the Hartmann number increase. For the value of Ra and γ considered, the core streamlines start to flatten at the top and bottom of the cavity, while the isotherms are almost parallel. This indicates that conduction is dominated, see Fig. 5. For high Rayleigh numbers, the flow and heat transfer regime is characterized by a thermally stratified core region and two thin boundary layers on the vertical walls, see Fig. 6(a). Also, as the Rayleigh number and magnetic field increase ($Ra = 10^5$ and $Ha = 10, 50$), stronger convective motion takes place and the core vortex breaks up into three

cells. There is also a weak distortion of the isotherms, as indicated in Fig. 6(b) and (c). This occurs at smaller inclination angles of the magnetic field ($\gamma = \pi/6$). This is in agreement with the results reported by Al-Najem et al. [28] for the case of natural convection in a two-dimensional square cavity filled with a viscous fluid with a transverse magnetic field.

Typical velocity profiles at the vertical walls, U_w for $Ra = 10^3$ and different values of γ and Ha are shown in Fig. 7. We observe that for a fixed value of Ha that the minimum of the wall velocity is attained when the magnetic field is in the vertical direction ($\gamma = \pi/2$). On the other hand, for $\gamma = \pi/4$ the wall velocity decreases as Ha increases. We observe that for all the values of Ra considered,

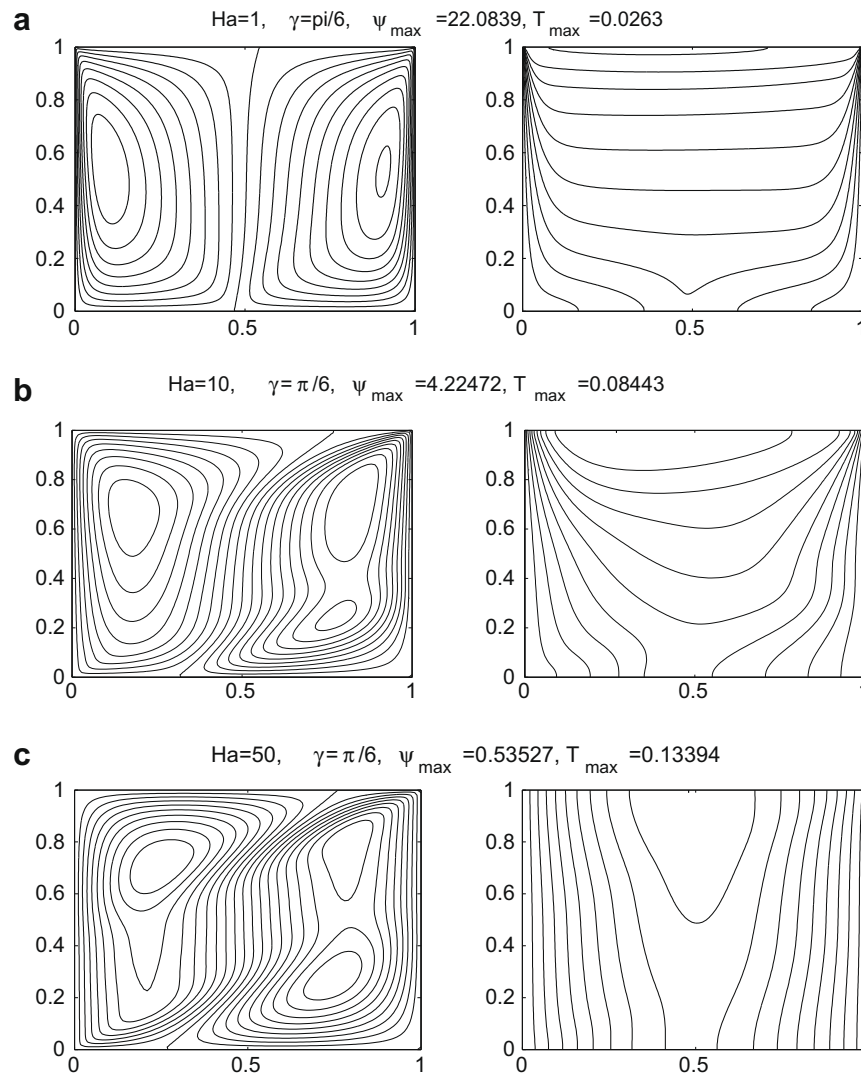


Fig. 6. Streamlines and isotherms for $Ra = 10^5$, $\gamma = \pi/6$ and for different values of Ha .

the maximum temperature profiles do not overshoot the limit prescribed by the analytical solution ($\theta_{\max} = 1/8$), see Fig. 8. Numerical and analytical solutions for the streamlines on the horizontal centerline plane of the cavity are shown in Fig. 9 for a small value of the aspect ratio, namely $a = 0.01$ and for $Ra = 10^3$ when $Ha = 0, 1, 5$ and $\gamma = 0$ (Fig. 9a) and when $Ha = 1$ and $\gamma = 0, \pi/4, \pi/2$ (Fig. 9b). We observe from these figures that there is very good agreement between the analytical and numerical solution.

Fig. 10 shows the variation of the local Nusselt number Nu_Y with Y for $Ra = 100$ and $\gamma = 0$. In order to compare the present results with those obtained by Haajizadeh et al. [27] when the magnetic field is absent ($Ha = 0$) the value of $2Nu_Y$ for $a = 0.2$ is presented in this figure. It is observed that the results are in very good agreement and therefore we are confident that the present results are accurate. Finally, Fig. 11 presents the variations of the local Nusselt number Nu_Y with Y for $Ra = 100$, $Ha = 1$ and for several values of γ when $a = 1$. It is also found that the local Nusselt number Nu_Y decreases at the bottom wall as γ increases (magnetic field changes its direction from the horizontal to the vertical direction) and vice versa for the top wall of the cavity.

6. Conclusion

The present numerical study exhibits many interesting features concerning the effect of the inclined magnetic fields on the free convection flow and heat transfer characteristics in a rectangular cavity filled with a porous medium. Detailed numerical results for the temperature distribution and heat transfer have been presented in graphical and tabular form. The main conclusions of the present analysis are as follows:

- In general, it has been found that the effect of the magnetic field is to reduce the convective heat transfer inside the cavity.
- The convection modes within the cavity were found to depend upon both the strength and the inclination of the magnetic field. The applied magnetic field in the horizontal direction was found to be most effective in suppressing the convection flow for a stronger magnetic field in comparison with the vertical direction.
- It is found that strong boundary layers are formed near the vertical walls for $Ra = 10^5$ and $\gamma = \pi/6$ and the intensity increases as Ha increases. The flat isotherms in the core region indicate that

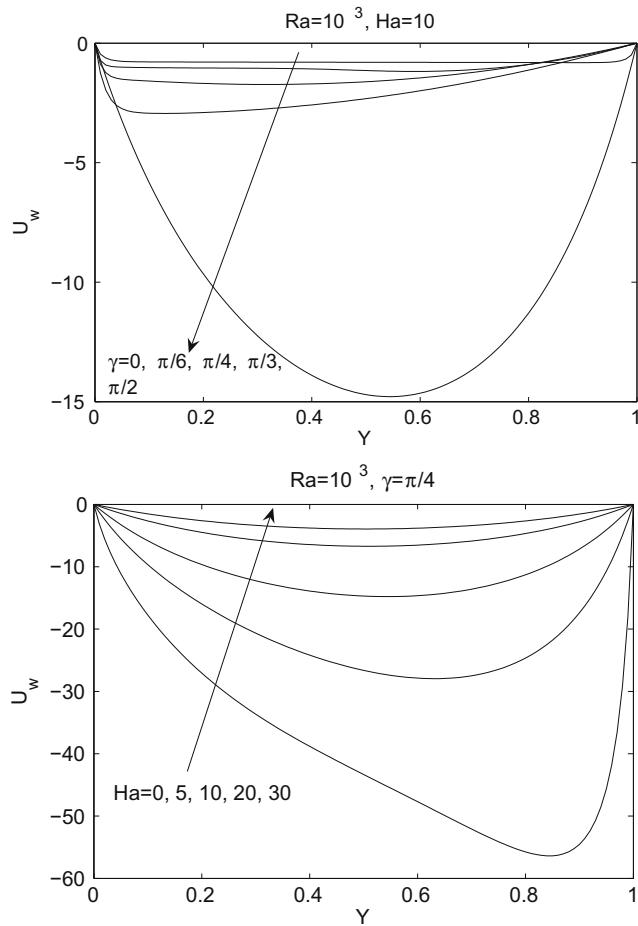


Fig. 7. The velocity profile in the vicinity of the vertical wall for different values of γ and Ha .

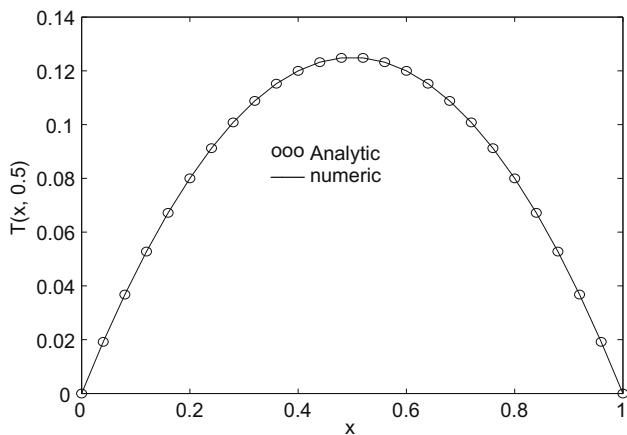


Fig. 8. Temperature profiles for $a = 0.01$ and $Ra = 10^3$.

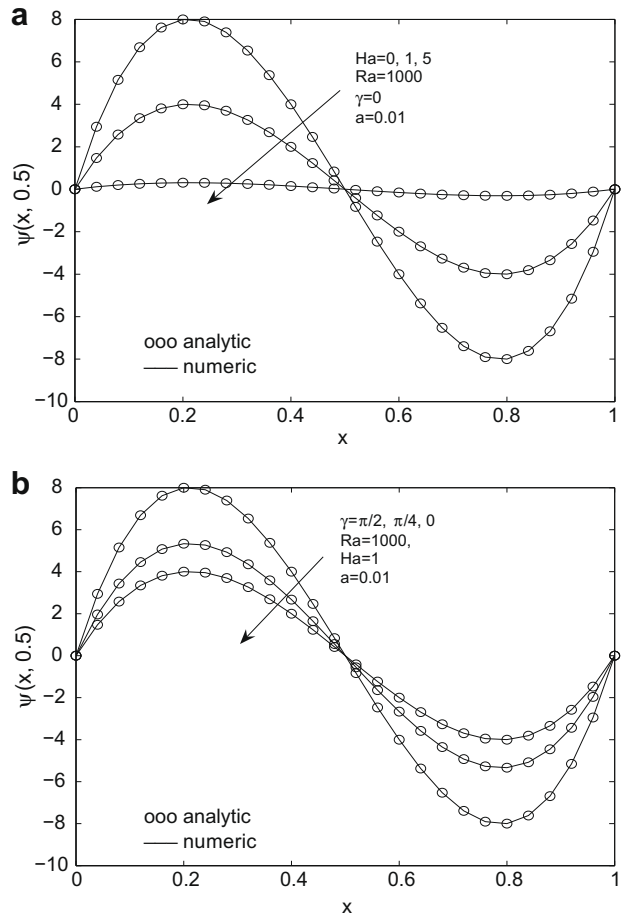


Fig. 9. Comparison between the streamlines obtained analytical and numerical: (a) for $\gamma = 0$ and different values of Ha ; (b) for $Ha = 1$ and different values of γ .

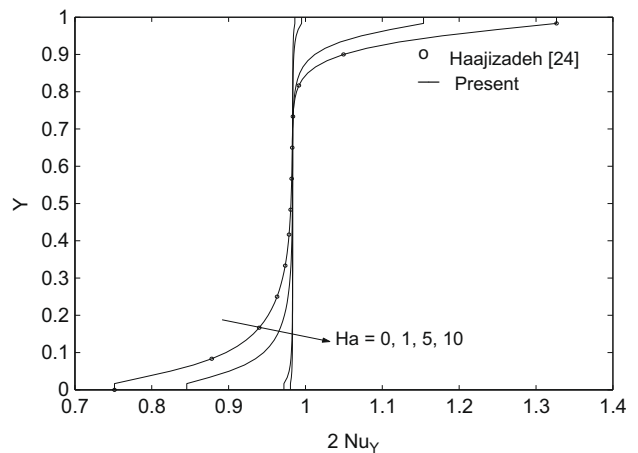


Fig. 10. Local Nusselt number for $Ra = 100$, $a = 0.2$, $\gamma = 0$ and different values of Ha .

there is negligible lateral heat conduction and the equal spacing of the streamlines implies a uniform vertical velocity in this region, as predicted by boundary layer theory, see Fig. 6(a).

- The magnetic field has a negligible effect on the heat transfer mechanism for small values of γ and $Ha \gg 1$. This is true since pure conduction becomes dominant when the magnetic field is applied in the horizontal direction ($\gamma = 0$). However, for $Ra = 10^5$ the parabolic profile is destroyed.

- For Rayleigh number $Ra = 10^3$, and small Hartmann numbers, the flow and heat transfer are characterized by a parallel flow structure in the central region of the cavity. The conduction is the dominant mode of heat transfer and vertical velocity profiles and temperatures are almost parabolic.
- It should be pointed out that the general analysis described in this work can represent a useful starting point to treat more complex problems, such as, for example, time-dependent flows.

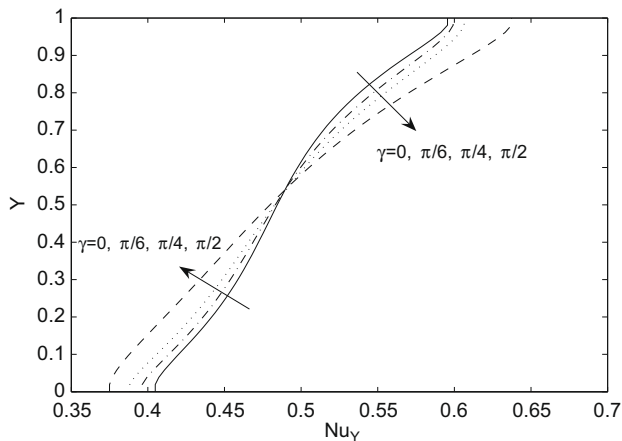


Fig. 11. Local Nusselt number for $Ra = 100$, $a = 1$, $Ha = 1$ and different values of γ .

Acknowledgements

The work done by T. Grosan and C. Revnic is supported by the MEDCT under Grant Ceex 90/2006. D.B. Ingham and I. Pop wishes to express their thanks to the Royal Society for partial financial support.

References

- [1] D.A. Nield, A. Bejan, *Convection in Porous Media*, third ed., Springer, New York, 2006.
- [2] D.B. Ingham, I. Pop (Eds.), *Transport Phenomena in Porous Media*, Elsevier, Oxford, 2005.
- [3] K. Vafai (Ed.), *Handbook of Porous Media*, second ed., Taylor & Francis, Boca Raton, FL, 2005.
- [4] A. Bejan, I. Dincer, S. Lorente, A.F. Miguel, A.H. Reis, *Porous and Complex Flows Structures in Modern Technologies*, Springer, New York, 2004.
- [5] I. Pop, D.B. Ingham, *Convective Heat Transfer: Mathematical and Computational Modelling of Viscous Fluids and Porous Media*, Pergamon Press, Oxford, 2001.
- [6] M.J.S. de Lemos, *Turbulence in Porous Media: Modeling and Applications*, Elsevier, Oxford, 2006.
- [7] P. Vadasz (Ed.), *Emerging Topics in Heat and Mass Transfer in Porous Media*, Springer, New York, 2008.
- [8] O. Martynenko, P. Khramtsov, *Free-Convective Heat Transfer*, Springer, Berlin, 2005.
- [9] S. Acharya, R.J. Goldstein, Natural convection in an externally heated vertical or inclined square box containing internal energy sources, *J. Heat Transfer* 107 (1985) 855–866.
- [10] H. Ozoe, K. Okada, The effect of the direction of the external magnetic field on the three-dimensional natural convection in cubical enclosure, *Int. J. Heat Mass Transfer* 32 (1989) 1939–1954.
- [11] J.-H. Lee, R.J. Goldstein, An experimental study on natural convection heat transfer in an inclined square enclosure containing internal energy sources, *J. Heat Transfer* 110 (1988) 345–349.
- [12] T. Fusegi, J.M. Hyun, K. Kuwahara, Natural convection in a differentially heated square cavity with internal heat generation, *Numer. Heat Transfer A* 21 (1992) 215–229.
- [13] M. Venkatachalla, C.K. Subbaraya, Natural convection in a rectangular enclosure in the presence of a magnetic field with uniform heat flux from the side walls, *Acta Mech.* 96 (1993) 13–26.
- [14] Y.M. Shim, J.M. Hyun, Transient confined natural convection with internal heat generation, *Int. J. Heat Fluid Flow* 18 (1997) 328–333.
- [15] M.A. Hossain, M. Wilson, Natural convection flow in a fluid-saturated porous medium enclosed by non-isothermal walls with heat generation, *Int. J. Therm. Sci.* 41 (2002) 447–454.
- [16] J.P. Garandet, T. Albussoiere, R. Moreau, Buoyancy driven convection in a rectangular enclosure with a transverse magnetic field, *Int. J. Heat Mass Transfer* 35 (1992) 741–748.
- [17] S. Alchaar, P. Vasseur, E. Bilgen, Natural convection heat transfer in a rectangular enclosure with a transverse magnetic field, *J. Heat Transfer* 117 (1995) 668–673.
- [18] K. Kanafer, A.J. Chamkha, Hydromagnetic natural convection from an inclined porous square enclosure with heat generation, *Numer. Heat Transfer A* 33 (1998) 891–910.
- [19] A.J. Chamkha, H. Al-Naser, Double-diffusive convection in an inclined porous enclosure with opposing temperature and concentration gradients, *Int. J. Therm. Sci.* 40 (2001) 227–244.
- [20] S. Mahmud, S.H. Tasnim, M.A.H. Mamun, Thermodynamic analysis of mixed convection in a channel with transverse hydromagnetic effect, *Int. J. Therm. Sci.* 42 (2003) 731–740.
- [21] M.A. Hossain, D.A.S. Rees, Natural convection flow of water near its density maximum in a rectangular enclosure having isothermal walls with heat generation, *Heat Mass Transfer* 41 (2005) 367–374.
- [22] M.A. Hossain, M.Z. Hafiz, D.A.S. Rees, Buoyancy and thermo capillary driven convection flow of an electrically conducting fluid in an enclosure with heat generation, *Int. J. Therm. Sci.* 44 (2005) 676–684.
- [23] M.C. Ece, E. Büyük, Natural-convection flow under a magnetic field in an inclined rectangular enclosure heated and cooled on adjacent walls, *Fluid Dyn. Res.* 38 (2006) 564–590.
- [24] D.A. Nield, Impracticality of MHD convection in a porous medium, *Transport Porous Med.* 73 (2008) 379–380.
- [25] A. Barletta, S. Lazzari, E. Magayri, I. Pop, Mixed convection with heating effect in a vertical porous annulus with a radially varying magnetic field, *Int. J. Heat Mass Transfer* 51 (25–26) (2008) 5777–5784.
- [26] G.D. Smith, *Numerical Solution of Partial Differential Equations: Finite Difference Method*, Oxford university Press, New York, 2004.
- [27] M. Haajizadeh, A.F. Ozguc, C.L. Tien, Natural convection in a vertical porous enclosure with internal heat generation, *Int. J. Heat Mass Transfer* 27 (1984) 1893–1902.
- [28] N.M. Al-Najem, K.M. Khanafer, M.M. El-Refae, Numerical study of laminar natural convection in tilted enclosure with transverse magnetic field, *Int. J. Numer. Methods Heat Fluid Flow* 8 (1998) 651–672.
- [29] V.J. Mandar, U.N. Gaitonde, K.M. Sushanta, Analytical study of natural convection in a cavity with volumetric heat generation, *J. Heat Transfer* 128 (2006) 176–182.